

Cite this: *Nanoscale*, 2011, **3**, 1984

www.rsc.org/nanoscale

PAPER

Ferrocene-functionalized carbon nanoparticles†

Yang Song, Xiongwu Kang, Nathaniel B. Zuckerman, Bruce Phebus, Joseph P. Konopelski and Shaowei Chen*

Received 6th December 2010, Accepted 20th January 2011

DOI: 10.1039/c0nr00953a

Carbon nanoparticles were synthesized from natural gas soot and functionalized with ferrocenyl moieties by using 4-ferrocenylphenyldiazonium as the reactive precursor. The incorporation of the ferrocenyl units onto the carbon nanoparticle surface was confirmed by varied spectroscopic measurements. For instance, in FTIR measurements the characteristic vibrational bands of the ferrocenyl and phenyl moieties could be clearly identified. XPS measurements showed that there were approximately 31.9 ferrocenyl units per nanoparticle. UV-vis spectroscopic measurements displayed an absorption band at *ca.* 465 nm which was consistent with the optical characteristics of ferrocenyl derivatives. Furthermore, with surface functionalization by the ferrocenyl moieties, the photoluminescence of the carbon nanoparticles was found to diminish in intensity and red-shift in energy with the addition of NOBF₄. This was accounted for by the formation of varied electron-accepting moieties on the particle surface, such as positively charged ferrocenium, quinone-like derivatives, and nitrosation of the aromatic rings of the graphitic cores. Interestingly, in electrochemical studies the nanoparticle-bound ferrocenyl moieties were found to exhibit two pairs of voltammetric waves with a difference of their formal potentials at about 78 mV, suggesting nanoparticle-mediated intraparticle charge delocalization at mixed valence as a result of the strong core–ligand covalent bonds and the conductive sp² carbon matrix of the graphitic cores. Consistent behaviors were observed in near-infrared measurements, indicating that the particles behaved analogously to a Class I/II mixed-valence compound.

Introduction

Carbon nanoparticles represent a unique form of carbon-based nanomaterials that, similar to their well-known cousins of fullerenes and carbon nanotubes, exhibit interesting optical and electronic properties that may be exploited for extensive applications in diverse areas.^{1,2} Typically, carbon nanoparticles are prepared by laser ablation of a graphitic target^{3,4} or by electrochemical treatments of carbon nanotubes.⁵ More recently it was demonstrated that nanosized carbon particles could also be produced by oxidative treatments of carbon soots which were collected from the incomplete combustion of candles or natural gas.^{6–8} High-resolution transmission electron microscopic (HRTEM) measurements showed that the as-produced nanoparticles exhibited a crystalline graphitic core with the core surface decorated with various oxygenated functional moieties where the quinone-like derivatives gave rise to unique

electrochemical and spectroscopic characteristics.^{7,8} By taking advantage of the chemical reactivity of carbon surfaces, it is anticipated that the material properties of carbon nanoparticles can be further manipulated by controlled chemical functionalization. This is the primary motivation of the present study.

It has been rather well-known that carbon surfaces can be readily functionalized by (electro)chemical grafting of diazonium derivatives, where a strong covalent C–C bond is formed between the functional ligand and the carbon substrate.^{9–12} Such a unique interfacial bonding interaction may be exploited to initiate intraparticle electronic coupling between particle-bound functional moieties, as the carbon nanoparticles exhibit a graphitic core with an sp² carbon network that serves as a conducting medium. It should be noted that the recent observation of nanoparticle-mediated electronic communication is primarily limited to transition-metal nanoparticles functionalized with conjugated metal–carbon covalent bonds at the metal–ligand interface such as Ru=carbene π bonds and Ru–C \equiv bonds.^{13–17} Therefore, chemically functionalized carbon nanoparticles offer a unique structural framework within which the impacts of the core–ligand interfacial bonding interactions on intraparticle charge delocalization and hence nanoparticle optical and electronic properties can be examined.

In the present study, we functionalized carbon nanoparticles with 4-ferrocenylphenyldiazonium and determined the surface

Department of Chemistry and Biochemistry, University of California, 1156 High Street, Santa Cruz, California, 95064, USA. E-mail: shaowei@ucsc.edu

† Electronic supplementary information (ESI) available: XPS spectra of the Fc-CNP sample and the corresponding UV-vis spectra after the nanoparticles were oxidized by NOBF₄, as well as square wave voltammograms and NIR spectra of the FcCH₂-CNP sample. See DOI: 10.1039/c0nr00953a

concentration by X-ray photoelectron spectroscopic (XPS) measurements. We then examined the impacts of ferrocenyl functionalization on the spectroscopic and electrochemical characteristics of the nanoparticles by exploiting the ferrocenyl moieties as the electrochemical probe and the photoluminescence characteristics of the carbon nanoparticles as the optical yardstick. The results suggest that electronic communication occurred between the nanoparticle-bound ferrocenyl moieties at mixed valence, although the electronic coupling was somewhat weak and consistent with the behaviors of Class I/II compounds as defined by Robin and Day.¹⁸ This indicates that, to a limited extent, the C(sp²)-C(sp²) interfacial bonding interactions offer a new pathway towards the manipulation of the chemical and physical properties of carbon nanoparticles. In contrast, with the insertion of an sp³ carbon spacer (CH₂) between the phenyl and ferrocenyl moieties, the ferrocenyl groups were found to behave independently, as reflected in electrochemical and spectroscopic measurements, indicating the effective turn-off of intraparticle charge delocalization by the saturated spacer.

Experimental section

Chemicals

Nitrosonium tetrafluoroborate (NOBF₄, 95%, Acros), tetrabutylammonium perchlorate (TBAP, 99%, Acros), superhydride (LiB(C₂H₅)₃H, 1 M in THF, Acros), sodium nitrite (NaNO₂, p.a., Acros), and fluoroboric acid (HBF₄, 50 wt% in water, Acros) were all used as received. 4-Ferrocenylaniline was synthesized and characterized by following a literature procedure.^{19,20} All solvents (e.g., dimethyl sulfoxide, DMSO) were obtained from typical commercial sources and used without further treatment. Water was supplied by a Barnstead Nanopure water system (18.3 MΩ cm).

Carbon nanoparticles (CNPs)

The preparation of carbon nanoparticles has been detailed previously.^{7,8} Briefly, carbon soot was collected on the inside wall of a glass beaker by placing the beaker upside-down above the flame of a natural gas burner. Typically 100 mg of the soot was then refluxed in 10 mL of 5 M HNO₃ for 12 h. When cooled down to room temperature, the brownish yellow supernatant after centrifugation was neutralized by Na₂CO₃, and then dialyzed against Nanopure water through a dialysis membrane for 3 days, affording purified carbon nanoparticles which exhibited an average core diameter of 4.8 ± 0.6 nm with well-defined graphitic crystalline lattices, as determined by high-resolution transmission electron microscopic measurements.^{7,8}

Synthesis of 4-ferrocenylphenyldiazonium

4-Ferrocenylphenyldiazonium was synthesized by following a synthetic protocol in the literature.²¹ Briefly, 50 mmol of 4-ferrocenylaniline was dissolved in 5 mL of ice-cold fluoroboric acid, into which a 1 : 1 stoichiometric amount of sodium nitrite was added. The solution was allowed to mix for 30 min. The obtained diazonium tetrafluoroborate salt was then thoroughly washed with cold fluoroboric acid, ethanol, and ether to remove excessive impurities, and used immediately to functionalize the

carbon nanoparticles prepared above. The procedure is detailed below.

Ferrocene-functionalized carbon nanoparticles (Fc-CNPs)

The 4-ferrocenylphenyldiazonium salt obtained above was added to 5 mL of an ice-cold solution of CNPs (6 mg mL⁻¹) in water under vigorous stirring for 30 min. 0.5 mL of superhydride was then added dropwise into the solution to initiate reduction of the diazonium compound. An equal amount of dichloromethane (DCM) was then added to the solution, and it was found that the organic phase became brownish in color whereas the aqueous phase colorless, signifying the formation of ferrocene-functionalized carbon nanoparticles and the transfer of the resulting particles into the organic phase. The water phase was separated and discarded, and repeated extraction with water was carried out to remove water-soluble by-products and excessive reactants from the DCM phase. After the container sat on the bench for a few days, black precipitates started to appear in the DCM phase, which were collected by centrifugation and extensively washed with DCM until the DCM phase was colorless. The purified nanoparticles were denoted as Fc-CNPs.

Spectroscopies

UV-vis spectroscopic studies were performed with an ATI Unicam UV4 spectrometer, and NIR spectra were acquired with an Ocean Optics NIR-512 spectrometer. In both measurements a 1 cm quartz cuvette was used. FTIR measurements were carried out with a Perkin-Elmer FTIR spectrometer (Spectrum One) where the samples were prepared by compressing the materials of interest into a KBr pellet. The spectral resolution was 4 cm⁻¹. Photoluminescence measurements were carried out with a PTI Fluorescence Spectrometer by using the same solutions as those for UV-vis and NIR studies. X-Ray photoelectron spectra (XPS) were recorded with a PHI 5400/XPS instrument equipped with an Al Kα source operated at 350 W and at 10⁻⁹ torr. Silicon wafers were sputtered by argon ions to remove carbon from the background and used as substrates. The spectra were charge-referenced to the Au 4f_{7/2} peak (83.8 eV) of sputtered gold.

Electrochemistry

Voltammetric measurements were carried out with a CHI 440 electrochemical workstation. A polycrystalline gold disk electrode (sealed in a glass tubing) was used as the working electrode. A Ag/AgCl wire and a Pt coil were used as the (quasi)reference and counter electrodes, respectively. The gold electrode was first polished with alumina slurries of 0.05 μm and then cleansed by sonication in 0.1 M HNO₃, H₂SO₄ and Nanopure water successively. Prior to data collection, the electrolyte solution was deaerated by bubbling ultrahigh-purity N₂ for at least 20 min and blanketed with a nitrogen atmosphere during the entire experimental procedure. The voltammograms were acquired both in the dark and with the electrochemical cell exposed to a UV light source (370 nm, 18 W).

Results and discussion

The incorporation of the ferrocenyl moieties onto the carbon nanoparticle surface was first confirmed by FTIR measurements.

Fig. 1 depicts the FTIR spectra of the carbon nanoparticles before and after reactions with 4-ferrocenylphenyldiazonium. In comparison with the spectral data of the as-prepared carbon nanoparticles (blue curve), several new features emerged for Fc-CNPs (black curve) which are consistent with the vibrational characteristics of the ferrocenyl and phenyl moieties,^{22,23} including 3068 cm^{-1} ($\nu_{\text{C-H}}$), 1600 cm^{-1} ($\nu_{\text{C=C}}$, phenyl), $1450\text{--}1506\text{ cm}^{-1}$ ($\nu_{\text{C=C}}$, ferrocenyl), 1018 cm^{-1} ($\delta_{\text{C-H}}$), and 820 cm^{-1} ($\pi_{\text{C-H}}$). These vibrational bands can also be clearly identified with monomeric 4-ferrocenylaniline (red curve). Note that the vibrational stretches of N-H ($\sim 3450\text{ cm}^{-1}$) and C-N (1295 cm^{-1}) are very well-defined with 4-ferrocenylaniline, and disappeared in the ferrocene-functionalized carbon nanoparticles, indicating that the Fc-CNP samples were free of excessive aniline monomers.

Furthermore, as reported previously,⁷ the as-prepared carbon nanoparticles exhibited various oxygenated species on the surface, which was manifested with the carbonyl vibrational band ($\nu_{\text{C=O}}$) at 1724 cm^{-1} . Interestingly, this band became weakened rather substantially with the Fc-CNP sample, most probably as a consequence of superhydride reduction during the ferrocene functionalization process (it is likely that the broad peak around 3400 cm^{-1} includes contributions from both the resulting hydroxy moieties as well as residual water).

The attachment of the ferrocenyl moieties onto the carbon nanoparticles was also manifested in XPS measurements (Fig. S1†). The C1s electrons can be clearly identified at 284.4 eV , consistent with the graphitic nature (sp^2 carbons) of the carbon nanoparticles;⁷ whereas the two peaks at 719.9 eV and 707.3 eV can be assigned to the $\text{Fe}2\text{p}_{1/2}$ and $\text{Fe}2\text{p}_{3/2}$ electrons of the ferrocenyl moieties.²⁴ Based on the integrated peak areas of the C1s and Fe2p electrons, the elemental ratio between of Fe and C in the Fc-CNP samples is estimated to be *ca.* 0.52% . By assuming a spherical structure of the graphitic core of the carbon nanoparticles (dia. $4.8 \pm 0.6\text{ nm}$),⁷ this corresponds to about 31.9 ferrocene moieties per nanoparticle, or a surface coverage of $7.32 \times 10^{-11}\text{ mol cm}^{-2}$. Note that this is significantly smaller than the saturated surface coverage of ferrocene-terminated self-assembled monolayers on gold surfaces ($3.2 \times 10^{-10}\text{ mol cm}^{-2}$).²⁵

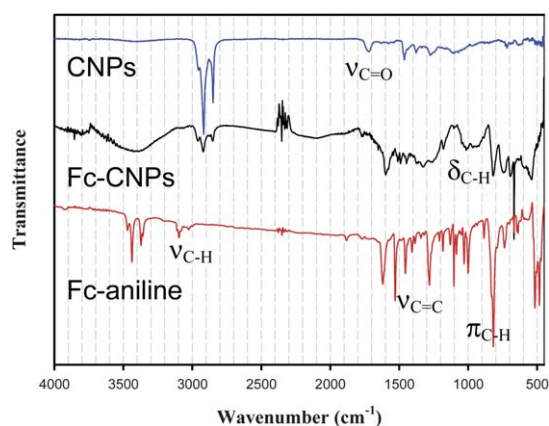


Fig. 1 FTIR spectra of the as-produced (CNPs, blue curve) and ferrocene-functionalized (Fc-CNPs, black curve) carbon nanoparticles, along with that for the monomeric 4-ferrocenylaniline (red curve).

The impacts of surface functionalization by the ferrocenyl moieties on the particle opto-electronic properties were then examined by electrochemical and spectroscopic measurements. Fig. 2(A) shows the square wave voltammograms (blue solid curve) of the Fc-CNP sample at a concentration of 6 mg mL^{-1} in DMSO with 0.1 M TBAP as the supporting electrolyte at a gold disk electrode in the dark. It can be seen that within the potential range of -0.2 to $+0.6\text{ V}$ there are two pairs of voltammetric peaks with the peak potentials at $+0.068\text{ V}$ and $+0.355\text{ V}$, respectively. The former can be ascribed to the charge transfer reactions of oxygenated functional moieties on the carbon nanoparticle surface that are analogous to phenanthraquinone derivatives, as observed previously with the as-prepared carbon nanoparticles,⁷ whereas the latter is attributable to the particle-bound ferrocenyl moieties that underwent one-electron oxidation to ferrocenium, $\text{Fc} \leftrightarrow \text{Fc}^+ + \text{e}$. In fact, consistent voltammetric profiles were observed with the ferrocenyl complexes produced by the reduction of 4-ferrocenylphenyldiazonium with superhydride (not shown). More interestingly, deconvolution of the experimental data shows that the broad ferrocenyl peak actually consists of two closely spaced voltammetric waves (green and red dashed curves) with the formal potentials (E°) at $+0.318\text{ V}$ and $+0.396\text{ V}$, respectively (note that the summation (black dashed curve) of these individual voltammetric profiles, along with that from the nanoparticle surface

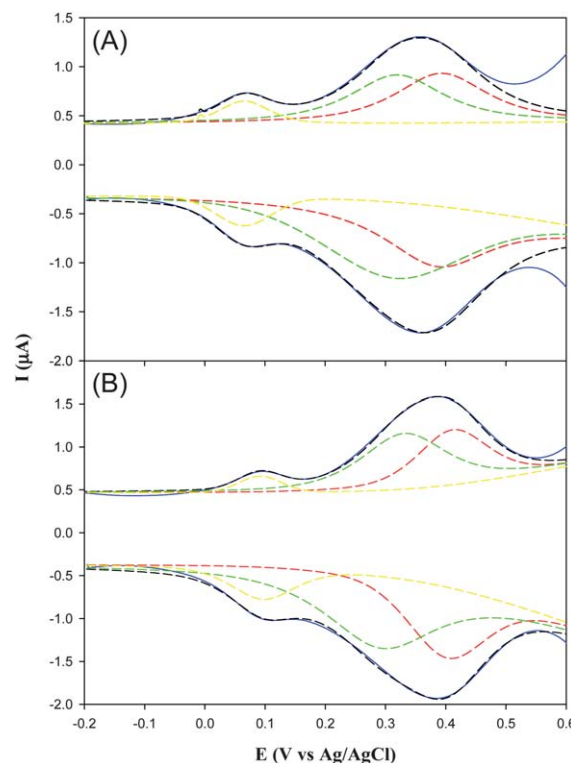


Fig. 2 Square wave voltammograms (SWVs) of ferrocene-functionalized carbon nanoparticles (Fc-CNPs) acquired (A) in the dark or (B) under UV photoirradiation (370 nm) at a gold electrode in 0.1 M tetrabutylammonium perchlorate (TBAP) in DMSO. Electrode surface area 2.63 mm^2 , particle concentration 6 mg mL^{-1} , increment of potential 4 mV , amplitude 25 mV and frequency 15 Hz . Solid curves are the experimental data and dashed lines represent the deconvolution of the voltammetric features.

species (yellow dashed curve), exhibits excellent agreement with the experimental data), and both of these two subpeaks exhibited a peak splitting (ΔE_p) less than 20 mV, consistent with the reversible kinetics of ferrocene electron-transfer reactions. This observation strongly suggests that intraparticle electronic communication occurred between the nanoparticle-bound ferrocenyl moieties at mixed valence, most probably as a result of the covalent grafting of the ferrocenyl ligands onto the graphitic particle cores where the sp^2 carbon matrix serves as a conducting medium for intraparticle charge delocalization. Yet the somewhat small difference of the formal potentials ($\Delta E^{\circ} = 78$ mV) indicates that the electronic coupling between the ferrocenyl metal centers is relatively weak. In fact, according to the classification by Robin and Day,¹⁸ the Fc-CNPs appeared to behave as a Class I/II compound.

It should be noted that the ferrocenyl moieties are covalently bridged by a spacer that consists of two phenylene units and a nanosized particle core. Despite this long chemical separation, intraparticle intervalence transfer between the particle-bound ferrocenyl moieties is resolvable voltammetrically. This is in contrast with a previous study²⁶ where methylated binuclear ferrocene derivatives bridged by a *p*-phenylene unit were found to exhibit two clearly reversible, one-electron voltammetric peaks with a potential spacing ranging from 70 to 120 mV, signifying apparent electronic communication between the ferrocenyl moieties; whereas the incorporation of a *p*-biphenylene spacer led to the appearance of a single reversible oxidation peak that corresponded to the simultaneous transfer of two electrons per dimer, indicating diminishment of the electronic coupling between the two ferrocenyl centers.

It should be noted that the surface coverage of the ferrocenyl moieties on the carbon nanoparticles was far less than a full monolayer (Fig. S1†). Thus the contribution of electrostatic (through-space) interactions to the appearance of intervalence transfer between the particle-bound ferrocenyl moieties at mixed valence is anticipated to be minimal. In other words, the observed intervalence transfer is most likely due to through-bond interactions, akin to those observed previously with Ru nanoparticles functionalized with Ru=carbene π bonds or Ru-C \equiv bonds.^{13–17}

This argument was further supported by the voltammetric data obtained when the Fc-CNP solution was exposed to UV (370 nm) photoirradiation, as manifested in Fig. 2(B). It can be seen that whereas the overall voltammetric features remained practically unchanged and two subpeaks can also be deconvoluted from the broad voltammetric wave at $\sim +0.40$ V, the potential separation (ΔE°) between these two subpeaks was found to increase to about 107 mV, suggesting that intraparticle charge delocalization might be facilitated by photoexcitation due to the photogenerated free electrons from the biphenylene bridge (*vide infra*). This is also consistent with the control experiment where an aniline derivative was synthesized with a CH_2 spacer inserted between the ferrocenyl and the phenylene moieties, *i.e.*, Fc- CH_2 - C_6H_4 - NH_2 , and the corresponding diazonium was used to functionalize the nanoparticles by using the same experimental procedure detailed in the Experimental section. The resulting nanoparticles (denoted as Fc CH_2 -CNPs) exhibited two pairs of voltammetric peaks in SWV measurements, and deconvolution could not resolve any additional peak (Fig. S2†),

no matter whether the voltammograms were acquired in the dark or under UV irradiation. The first peak at $E^{\circ} = +0.071$ V is almost the same as that observed with Fc-CNP (Fig. 2), which was, again, ascribed to the charge transfer reactions of oxygenated functional moieties on the carbon nanoparticle surface; whereas the second peak at $E^{\circ} = +0.240$ V was attributed to the redox reactions of nanoparticle-bound ferrocenyl moieties. The fact that only one pair of voltammetric peaks was observed for the ferrocenyl moieties in Fc CH_2 -CNP whereas two pairs for the Fc-CNP sample strongly discounts the hypothesis that the latter was a result of different binding sites on the CNP surface. Instead, the discrepancy of the voltammetric behaviors between these two nanoparticle samples strongly suggests that the intraparticle charge delocalization might be effectively turned off by the insertion of an sp^3 carbon spacer, consistent with our earlier studies with Ru nanoparticles.^{13–17}

The notion that electronic coupling occurred between the nanoparticle-bound ferrocenyl moieties at mixed valence was also manifested in near-infrared (NIR) spectroscopic measurements by using $NOBF_4$ as the oxidizing reagent. Fig. 3 shows the NIR absorption spectra of Fc-CNPs in DMSO with the addition of varied amounts of freshly prepared $NOBF_4$. It can be seen that with the addition of $NOBF_4$, two prominent absorption bands started to emerge at 1454 and 1950 nm, and as depicted in the figure inset, their peak intensities exhibited volcano-shaped dependency on the amount of $NOBF_4$ added, which is analogous to the unique NIR features of biferrocene derivatives at mixed valence. In sharp contrast, the NIR profile of the Fc CH_2 -CNP sample remained practically unchanged with the addition of a comparable amount of $NOBF_4$ (Fig. S3†).

These behaviors are consistent with the results in our previous studies where nanoparticle-mediated intraparticle intervalence transfer was observed with functional moieties bound onto metal nanoparticle surfaces by conjugated metal-carbon covalent bonds.^{13–17,27} For instance, previously we observed that when ferrocenyl moieties were bound onto Ru nanoparticle surface by a Ru=C π bond or Ru-C \equiv bond, two pairs of voltammetric

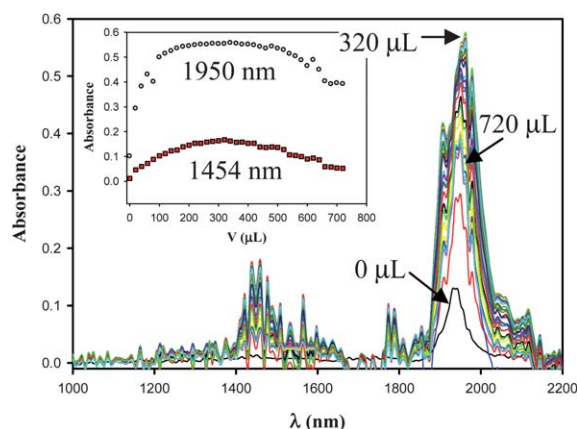


Fig. 3 Near-infrared (NIR) spectra of ferrocene-functionalized carbon nanoparticles (Fc-CNPs) with the addition of varied amounts of $NOBF_4$ in DMSO. The starting solution of the carbon nanoparticles was 2 mL at a concentration of 0.1 mM, and the concentration of the $NOBF_4$ solution was 5 mM. Totally 720 μ L $NOBF_4$ was added to the solution at an increment of 20 μ L. Inset shows the variation of the absorbances at 1454 nm and 1950 nm with the amounts of $NOBF_4$ added.

peaks appeared with a potential spacing of about 200 mV, rendering the nanoparticle materials to behave as Class II compounds. The much smaller ΔE^{ov} observed above with Fc-CNPs suggests that the C(sp², graphitic)–C(sp², phenyl) interfacial bonding interactions exhibit a much lower bonding order and therefore are less efficient in facilitating intraparticle charge delocalization. With an increase of the bonding order by photoirradiation with UV lights, enhanced electronic communication was observed between the particle-bound ferrocenyl moieties (Fig. 2(B)).

The optical properties of the ferrocenyl-functionalized nanoparticles (Fc-CNPs) were then examined by UV-vis and photoluminescence spectroscopic measurements. Fig. 4 depicts the UV-vis absorption spectra of the carbon nanoparticles before (blue curve) and after (red curve) ferrocenyl functionalization, along with that for 4-ferrocenylaniline (black curve). It can be seen that the original carbon nanoparticles exhibited a broad peak at around 365 nm, which was ascribed to the quinone-like functional moieties, such as 9,10-phenanthraquinone, on the nanoparticle surface.^{7,8} By contrast, after ferrocene functionalization, this peak essentially disappeared, suggesting the effective removal of the quinone-like functional moieties from the nanoparticle surface by superhydride, which is consistent with results from the FTIR measurements (Fig. 1).^{7,8} Furthermore, in comparison with the absorption profile of monomeric 4-ferrocenylaniline, three absorption peaks can be identified with Fc-CNPs, corresponding to the π – π^* (260 nm) and d–d (294 nm and 465 nm) electronic transitions that are characteristic of the ferrocenyl moiety.²⁸

The corresponding photoluminescence spectra of the carbon nanoparticles were then presented in Fig. 5. It can be seen that the original CNPs in water (black curves) exhibit a very well-defined excitation peak at 330 nm and an emission peak at 440 nm, as observed previously, which was accounted for by the electronic transitions of functional species on the nanoparticle surface.^{7,8} However, after ferrocenyl functionalization (red curves), the nanoparticles became soluble in DMSO and exhibited a substantial red-shift of the excitation peak to 376 nm and a small shift of the emission peak to 448 nm. Remarkably,

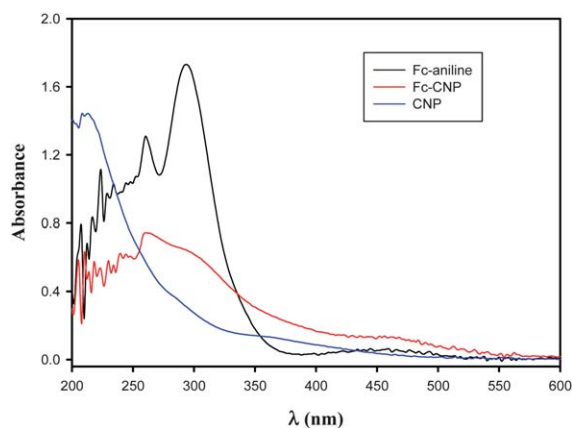


Fig. 4 UV-vis spectra of the as-produced (CNPs) and ferrocene-functionalized (Fc-CNPs) carbon nanoparticles, as well as the monomeric 4-ferrocenylaniline. The CNPs were dispersed in water whereas the Fc-CNP and Fc-aniline samples were in DMSO.

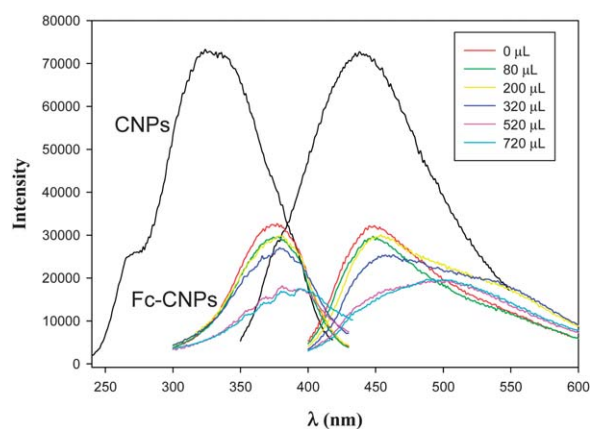


Fig. 5 Photoluminescence spectra of the as-produced (CNPs) and ferrocene-functionalized (Fc-CNPs) carbon nanoparticles. The solutions were the same as those in Fig. 3 and 4.

the resulting photoluminescence characteristics are very similar to those observed with conjugated organic oligo biphenylene vinylene molecules based on biphenylene motifs linked together through double bonds.²⁹ This observation is in agreement with the above argument that apparent electronic coupling occurred between the particle-bound ferrocenyl moieties because the chemical bridge that covalently connected these ferrocenyl groups behaved equivalently to a conjugated biphenylene unit, as manifested in the voltammetric and NIR measurements (Fig. 2 and 3). Furthermore, as the chemical bridge serves as the photoactive site, the molecular conductance may be enhanced by photoirradiation, leading to improved intraparticle charge delocalization, as observed experimentally (Fig. 2).

Interestingly, the Fc-CNP photoluminescence properties can be further manipulated by the charge state of the peripheral ferrocenyl units. From Fig. 5, it can be seen that the excitation (λ_{ex}) and emission (λ_{em}) peak positions exhibited an insignificant variation when the amount of NOBF₄ added was less than 320 μ L, where less than half of the ferrocenyl sites were oxidized to positively charged ferrocenium (Fig. 4). Further additions of NOBF₄ led to a rather drastic red-shift for both λ_{ex} and λ_{em} . For instance, when the ferrocenyl moieties were fully oxidized (720 μ L), the excitation peak (λ_{ex}) shifted to 393 nm and the emission profile became broadened significantly with the center of the peak (λ_{em}) moved to 502 nm. Concurrently, the fluorescence intensity diminished with the oxidative conversion of ferrocene into ferrocenium. These observations may again be accounted for by the nanoparticle-mediated electronic coupling between the peripheral ferrocenyl moieties. Specifically, the positively charged ferrocenium sites most likely (i) served as electron acceptors and thus quenched the fluorescence emitted from the biphenylene chemical spacer, and (ii) helped stabilize the photoexcited electrons by virtue of intraparticle charge delocalization which lowered the energy of the nanoparticle excited states and hence red-shift of the electronic transitions, as observed experimentally.

Additional contributions to the manipulation of the nanoparticle photoluminescence probably arose from the nitrosation of the aromatic rings of the nanoparticle graphitic cores as well as the formation of quinone-like derivatives by the oxidation of

hydroxyl species on the particle surface by NOBF₄, as both have been known to behave as efficient electron acceptors.^{8,30,31} In fact, upon the addition of NOBF₄, UV-vis measurements of the Fc-CNP nanoparticle solution showed that the absorption peak at 365 nm re-emerged and the intensity increased with the amount of NOBF₄ added (Fig. S4†).

Conclusion

Ferrocenyl-functionalized carbon nanoparticles were prepared by covalent grafting of 4-ferrocenylphenyldiazonium onto the nanoparticle surface. FTIR measurements confirmed the successful attachment of the ferrocenyl moieties onto the nanoparticle surface and XPS measurements showed that there were *ca.* 31.9 ferrocenyl moieties per nanoparticle. Interestingly, apparent electronic coupling between the nanoparticle-bound ferrocenyl moieties was observed in voltammetric measurements, where two pairs of voltammetric waves were identified with a potential spacing of about 78 mV, signifying that the nanoparticles behaved as a Class I/II compound, as defined by Robin and Day. Further supporting evidence was manifested in NIR measurements where two prominent peaks started to emerge at 1454 nm and 1950 nm with the addition of NOBF₄ that oxidized the peripheral ferrocenyl moieties into ferrocenium, and the peak intensities displayed volcano-shaped dependence on the amount of NOBF₄ added, indicating intraparticle intervalence transfer at mixed valence. These results strongly suggest that by virtue of the C(sp²)-C(sp²) interfacial bonding contacts, a rather delocalized chemical bridge was established between the nanoparticle-bound ferrocenyl units, which might be further enhanced by UV photoirradiation of the nanoparticle solution, with the potential spacing found to increase to 107 mV. Because of the nanoparticle-mediated charge delocalization, the particle photoluminescence characteristics were found to be further manipulated by the charge states of the peripheral ferrocenyl moieties. This study suggests that surface chemical functionalization may be exploited as an effective mechanism in the manipulation of nanomaterials optical and electronic properties.

Acknowledgements

This work was supported in part by the National Science Foundation through grants CHE-0832605 and CHE-0718170/CHE-1012258. XPS data were acquired at the Molecular Foundry, Lawrence Berkeley National Laboratory which is supported by the US Department of Energy.

References

- 1 M. S. Dresselhaus and G. Dresselhaus, *Nanostruct. Mater.*, 1997, **9**, 33.
- 2 M. S. Dresselhaus, *Annu. Rev. Mater. Sci.*, 1997, **27**, 1.
- 3 S. L. Hu, K. Y. Niu, J. Sun, J. Yang, N. Q. Zhao and X. W. Du, *J. Mater. Chem.*, 2009, **19**, 484.
- 4 Y. P. Sun, B. Zhou, Y. Lin, W. Wang, K. A. S. Fernando, P. Pathak, M. J. Meziani, B. A. Harruff, X. Wang, H. F. Wang, P. J. G. Luo, H. Yang, M. E. Kose, B. L. Chen, L. M. Veca and S. Y. Xie, *J. Am. Chem. Soc.*, 2006, **128**, 7756.
- 5 J. G. Zhou, C. Booker, R. Y. Li, X. T. Zhou, T. K. Sham, X. L. Sun and Z. F. Ding, *J. Am. Chem. Soc.*, 2007, **129**, 744.
- 6 H. P. Liu, T. Ye and C. D. Mao, *Angew. Chem., Int. Ed.*, 2007, **46**, 6473.
- 7 L. Tian, D. Ghosh, W. Chen, S. Pradhan, X. J. Chang and S. W. Chen, *Chem. Mater.*, 2009, **21**, 2803.
- 8 L. Tian, Y. Song, X. J. Chang and S. W. Chen, *Scr. Mater.*, 2010, **62**, 883.
- 9 J. Pinson and F. Podvorica, *Chem. Soc. Rev.*, 2005, **34**, 429.
- 10 R. L. McCreery, *ChemPhysChem*, 2009, **10**, 2387.
- 11 M. S. Strano, A. A. Boghossian, W. J. Kim, P. W. Barone, E. S. Jeng, D. A. Heller, N. Nair, H. Jin, R. Sharma and C. Y. Lee, *MRS Bull.*, 2009, **34**, 950.
- 12 J. M. Seiberg, M. Kullapere, U. Maeorg, F. C. Maschion, G. Maia, D. J. Schiffrin and K. Tammeveski, *J. Electroanal. Chem.*, 2008, **624**, 151.
- 13 W. Chen, S. W. Chen, F. Z. Ding, H. B. Wang, L. E. Brown and J. P. Konopelski, *J. Am. Chem. Soc.*, 2008, **130**, 12156.
- 14 W. Chen, L. E. Brown, J. P. Konopelski and S. W. Chen, *Chem. Phys. Lett.*, 2009, **471**, 283.
- 15 W. Chen, N. B. Zuckerman, J. W. Lewis, J. P. Konopelski and S. W. Chen, *J. Phys. Chem. C*, 2009, **113**, 16988.
- 16 W. Chen, N. B. Zuckerman, J. P. Konopelski and S. W. Chen, *Anal. Chem.*, 2010, **82**, 461.
- 17 W. Chen, N. B. Zuckerman, X. W. Kang, D. Ghosh, J. P. Konopelski and S. W. Chen, *J. Phys. Chem. C*, 2010, **114**, 18146.
- 18 M. B. Robin and P. Day, *Adv. Inorg. Chem. Radiochem.*, 1967, **10**, 247.
- 19 P. Hu, K. Q. Zhao and H. B. Xu, *Molecules*, 2001, **6**, M249.
- 20 P. Hu, K. Q. Zhao and H. B. Xu, *Molecules*, 2001, **6**, M250.
- 21 H. H. Yang and R. L. McCreery, *Anal. Chem.*, 1999, **71**, 4081.
- 22 Y. K. Gun'ko, T. S. Perova, S. Balakrishnan, A. A. Potapova, R. A. Moore and E. V. Astrova, *Phys. Status Solidi A*, 2003, **197**, 492.
- 23 L. H. Guan, Z. J. Shi, M. X. Li and Z. N. Gu, *Carbon*, 2005, **43**, 2780.
- 24 C. D. Wagner, W. M. Riggs, L. E. Davis, J. F. Moulder and G. E. Muilenberg, *Handbook of X-Ray Photoelectron Spectroscopy: a Reference Book of Standard Data for Use in X-ray Photoelectron Spectroscopy*, Perkin-Elmer Corp., 1979.
- 25 H. C. Delong, J. J. Donohue and D. A. Buttry, *Langmuir*, 1991, **7**, 2196.
- 26 E. E. Bunel, P. Campos, J. Ruz, L. Valle, I. Chadwick, M. S. Ana, G. Gonzalez and J. M. Manriquez, *Organometallics*, 1988, **7**, 474.
- 27 X. W. Kang, N. B. Zuckerman, J. P. Konopelski and S. W. Chen, *Angew. Chem., Int. Ed.*, 2010, **49**, 9496.
- 28 Y. S. Sohn, D. N. Hendrickson, J. H. Smith and H. B. Gray, *Chem. Phys. Lett.*, 1970, **6**, 499.
- 29 F. Lincker, P. Bourgun, P. Masson, P. Didier, L. Guidoni, J. Y. Bigot, J. F. Nicoud, B. Donnio and D. Guillon, *Org. Lett.*, 2005, **7**, 1505.
- 30 H. Johnson and E. Sawicki, *Talanta*, 1966, **13**, 1361.
- 31 N. V. Zyk, E. E. Nesterov, A. N. Khlobystov and N. S. Zefirov, *Russ. Chem. Bull.*, 1999, **48**, 506.